

AD 745425

Sec 744821

## Computer Modeling and Parametric Study for a Pulsed $H_2 + F_2$ Laser

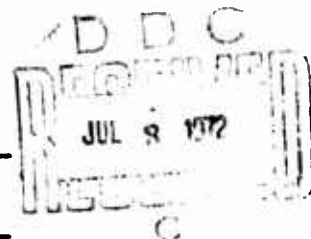
Prepared by R. L. KERBER, G. EMANUEL, and J. S. WHITTIER  
Aerodynamics and Propulsion Research Laboratory

72 JUN 86

---

Laboratory Operations  
THE AEROSPACE CORPORATION

---



Prepared for SPACE AND MISSILE SYSTEMS ORGANIZATION  
AIR FORCE SYSTEMS COMMAND  
LOS ANGELES AIR FORCE STATION  
Los Angeles, California

Reproduced by  
NATIONAL TECHNICAL  
INFORMATION SERVICE  
U S Department of Commerce  
Springfield VA 22151

APPROVED FOR PUBLIC RELEASE:  
DISTRIBUTION UNLIMITED

## LABORATORY OPERATIONS

The Laboratory Operations of The Aerospace Corporation is conducting experimental and theoretical investigations necessary for the evaluation and application of scientific advances to new military concepts and systems. Versatility and flexibility have been developed to a high degree by the laboratory personnel in dealing with the many problems encountered in the nation's rapidly developing space and missile systems. Expertise in the latest scientific developments is vital to the accomplishment of tasks related to these problems. The laboratories that contribute to this research are:

**Aerodynamics and Propulsion Research Laboratory:** Launch and reentry aerodynamics, heat transfer, reentry physics, propulsion, high-temperature chemistry and chemical kinetics, structural mechanics, flight dynamics, atmospheric pollution, and high-power gas lasers.

**Electronics Research Laboratory:** Generation, transmission, detection, and processing of electromagnetic radiation in the terrestrial and space environments, with emphasis on the millimeter-wave, infrared, and visible portions of the spectrum; design and fabrication of antennas, complex optical systems, and photolithographic solid-state devices; test and development of practical superconducting detectors and laser devices and technology, including high-power lasers, atmospheric pollution, and biomedical problems.

**Materials Sciences Laboratory:** Development of new materials; metal matrix composites and new forms of carbon; test and evaluation of graphite and ceramics in reentry; spacecraft materials and components in radiation and high-vacuum environments; application of fracture mechanics to stress corrosion and fatigue-induced fractures in structural metals; effect of nature of material surfaces on lubrication, photosensitization, and catalytic reactions; and development of prosthesis devices.

**Plasma Research Laboratory:** Reentry physics and nuclear weapons effects; the interaction of antennas with reentry plasma sheaths; experimentation with thermonuclear plasmas; the generation and propagation of plasma waves in the magnetosphere; chemical reactions of vibrationally excited species in rocket plumes; and high-precision laser ranging.

**Space Physics Laboratory:** Aeronomy, density and composition of the atmosphere at all altitudes; atmospheric reactions and atmospheric optics; pollution of the environment; the sun, earth's resources; meteorological measurements; radiation belts and cosmic rays; and the effects of nuclear explosions, magnetic storms, and solar radiation on the atmosphere.

THE AEROSPACE CORPORATION  
El Segundo, California

REF ID: A66010		WHITE SECTION <input checked="" type="checkbox"/>	
UNCLASSIFIED		DIFF. SECTION <input type="checkbox"/>	
JUSTIFICATION			
BY			
DISTRIBUTION/AVAILABILITY CODES			
DIST.	AVAIL.	SPECIAL	
A			

UNCLASSIFIED

Security Classification

DOCUMENT CONTROL DATA - R & D		
(Security classification of title, body of abstract and indexing annotation must be entered when the overall report is classified)		
1. ORIGINATING ACTIVITY (Corporate author)		2a. REPORT SECURITY CLASSIFICATION
The Aerospace Corporation El Segundo, California		Unclassified
		2b. GROUP
3. REPORT TITLE		
COMPUTER MODELING AND PARAMETRIC STUDY FOR A PULSED H <sub>2</sub> + F <sub>2</sub> LASER		
4. DESCRIPTIVE NOTES (Type of report and inclusive dates)		
5. AUTHOR(S) (First name, middle initial, last name)		
Ronald L. Kerber, George Emanuel, and James S. Whittier		
6. REPORT DATE	7a. TOTAL NO. OF PAGES	7b. NO. OF REFS
72 JUN 06	49	11
8a. CONTRACT OR GRANT NO.	9a. ORIGINATOR'S REPORT NUMBER(S)	
F04701-71-C-0172	TR-0172(2573)-3	
b. PROJECT NO.		
c.	9b. OTHER REPORT NO(S) (Any other numbers that may be assigned this report)	
d.	SAMSO-TR-72-140	
10. DISTRIBUTION STATEMENT		
Approved for public release; distribution unlimited.		
11. SUPPLEMENTARY NOTES		12. SPONSORING MILITARY ACTIVITY
		Space and Missile Systems Organization Air Force Systems Command Los Angeles, California
13. ABSTRACT		
<p>A computer simulation of a pulsed HF laser pumped by the H<sub>2</sub> + F<sub>2</sub> chain reaction is presented. A chemical kinetic model encompassing 68 reactions is used to approximate the reacting mixture contained within an optical cavity. For each vibrational level, a Boltzmann distribution for the rotational levels is assumed with lasing on the vibrational band at line center of the transition having maximum gain.</p> <p>An analysis of cavity and chemical mechanisms yields a simple relationship between the pumping and depletion rates of the vibrational levels. This relationship is used to make a comprehensive study of the effects of cavity and chemical parameters on the laser pulse. The effect of changes in uncertain chemical reaction rate coefficients is assessed. A competition exists between vibration-translation deactivation reactions and stimulated emission. Laser performance is most sensitive to the relative rates of the vibrational-translational and pumping reactions. In addition, the effect of the photon flux on the chemical mechanisms is significant.</p>		

La

UNCLASSIFIED

Security Classification

10

KEY WORDS

Chemical laser modeling

Pulsed laser

Fluorine plus hydrogen laser

Distribution Statement (Continued)

Abstract (Continued)

IL

UNCLASSIFIED

Security Classification

Air Force Report No.  
SAMSO-TR-72-140

Aerospace Report No.  
TR-0172(2753)-3

COMPUTER MODELING AND PARAMETRIC STUDY  
FOR A PULSED  $H_2 + F_2$  LASER

Prepared by  
R. L. Kerber, G. Emanuel, and J. S. Whittier  
Aerodynamics and Propulsion Research Laboratory

72 JUN 06

Laboratory Operations  
THE AEROSPACE CORPORATION

Prepared for  
SPACE AND MISSILE SYSTEMS ORGANIZATION  
AIR FORCE SYSTEMS COMMAND  
LOS ANGELES AIR FORCE STATION  
Los Angeles, California

Approved for public release;  
distribution unlimited

IC


## FOREWORD

This work reflects research supported by the Advanced Research Projects Agency of the Department of Defense under U.S. Air Force Space and Missile Systems Organization (SAMSO) Contract No. F04701-71-C-0172.

This report, which documents research carried out from December 1970 to June 1971, was submitted 13 March 1972 to Captain Karl J. Hoch, SYAE, for review and approval.

The authors gratefully acknowledge the efforts of D. W. Adams and E. B. Turner of the Information Processing Division of The Aerospace Corporation for the development of the computer program RESALE-1, used for the calculations presented here. The authors would also like to thank J. S. Lesser for her assistance in making the calculations.

Approved

  
\_\_\_\_\_  
W. R. Warren, Jr., Director  
Aerodynamics and Propulsion Research  
Laboratory

Publication of this report does not constitute Air Force approval of the report's findings or conclusions. It is published only for the exchange and stimulation of ideas.

  
\_\_\_\_\_  
Karl J. Hoch  
Captain, United States Air Force  
Project Officer

## ABSTRACT

A computer simulation of a pulsed HF laser pumped by the  $\text{H}_2 + \text{F}_2$  chain reaction is presented. A chemical kinetic model encompassing 68 reactions is used to approximate the reacting mixture contained within an optical cavity. For each vibrational level, a Boltzmann distribution for the rotational levels is assumed with lasing on the vibrational band at line center of the transition having maximum gain.

An analysis of cavity and chemical mechanisms yields a simple relationship between the pumping and depletion rates of the vibrational levels. This relationship is used to make a comprehensive study of the effects of cavity and chemical parameters on the laser pulse. The effect of changes in uncertain chemical reaction rate coefficients is assessed. A competition exists between vibration-translation deactivation reactions and stimulated emission. Laser performance is most sensitive to the relative rates of the vibrational-translational and pumping reactions. In addition, the effect of the photon flux on the chemical mechanisms is significant.

## CONTENTS

FOREWORD .....	ii
ABSTRACT .....	iii
NOMENCLATURE .....	ix
I. INTRODUCTION .....	1
II. THE CHEMICAL LASER COMPUTER SIMULATION .....	5
III. MECHANISMS OF THE PULSED HF LASER .....	9
A. General Energy Interpretation .....	9
B. A Detailed Interpretation of Mechanisms for the Standard Case .....	15
IV. PARAMETRIC VARIATION .....	23
A. Threshold .....	23
B. Diluents .....	26
C. Initial F <sub>2</sub> Dissociation .....	29
D. Initial Temperature .....	32
E. Initial H <sub>2</sub> Concentration .....	32
F. Variation of Important Rate Constants .....	32
V. CHEMICAL EFFICIENCY .....	37
VI. SUMMARY AND CONCLUSIONS .....	39
REFERENCES .....	41
APPENDIX. THE REACTION SYSTEM .....	A-1

**Preceding page blank**



## FIGURES

1.	Power History of the Standard Case . . . . .	10
2.	Laser Power and Energy Emission Rate . . . . .	11
3.	Time Histories of the Concentrations of $H_2$ , $F_2$ , $H$ , and $F$ for the Standard Case . . . . .	12
4.	Relationship of Dominant Mechanisms for the 2-1 Band of HF in a Chemical Laser . . . . .	14
5.	Production and Reduction Mechanisms for the Gain of the 2-1 Line . . . . .	16
6.	Temperature History of the Standard Case, with and without Radiation Suppressed . . . . .	18
7.	Gain History for Standard Case with Radiation Suppressed . . . . .	19
8.	Mechanisms Producing and Reducing F-Atom Concentration for the Standard Case . . . . .	21
9.	Time Histories of Important Rate Coefficients for the Standard Case . . . . .	22
10.	Effect of Threshold Gain on Pulse Energy . . . . .	24
11.	Effect of Threshold Gain on $t_1$ and $t_{1/2}$ . . . . .	25
12.	Effect of Diluent Concentration on Pulse Energy with Two Different Initial F-Atom Concentrations . . . . .	27
13.	Effect of Diluent Concentration on $t_{1/2}$ and $t_1$ . . . . .	28
14.	Effect of Initial $F_2$ Dissociation on Pulse Length . . . . .	30
15.	Effect of Initial $F_2$ Dissociation on Pulse Energy . . . . .	31

## FIGURES (cont.)

16.	Effect of Initial Temperature . . . . .	33
17.	Effect of Initial H <sub>2</sub> Concentration . . . . .	34

## TABLES

1.	Effect of Rate Changes on Pulse Characteristics . . . . .	36
----	---	----

## NOMENCLATURE

$B(v, J)$	Einstein isotropic absorption coefficient
$c$	speed of light, $2.9979 \times 10^{10}$ cm/sec
$C_{pi}$	specific heat at constant pressure of species $i$
$D_{v+1, v}$	chemical deactivation rate from level $v + 1$ to $v$
$E_L(t)$	energy emitted during laser pulse to time $t$
$E_J^v$	rotational energy associated with vibrational level $v$ and rotational level $J$
$E_{v+1, v}$	total energy emitted during lasing on a $v + 1 \rightarrow v$ band
$h$	Planck's constant, $6.6256 \times 10^{-34}$ joule-sec
$H_i$	molar enthalpy of species $i$
$J$	rotational quantum number
$J_L$	rotational quantum number associated with the lower level of a lasing transition
$k$	Boltzmann's constant, $1.3805 \times 10^{-23}$ joule/ $^{\circ}$ K
$k_n, k_{fr}$	forward rate coefficients
$k_{-n}, k_{br}$	backward rate coefficients
$L$	length of active medium
$L_{fr}, L_{br}$	forward and backward rates for reaction $r$
$M_j$	catalytic species of type $j$

$N_A$	Avogadro's number, $6.0225 \times 10^{23}$ molecules/mole
$N_i$	molar concentration of species $i$
$N(v)$	molar concentration of lasing species with vibrational level $v$
$N(v, J)$	molar concentration of lasing species with vibrational level $v$ and rotational level $J$
$p$	pressure
$p_i$	initial pressure of the reacting mixture
$P_L$	output power
$P_{v+1, v}$	output power for lasing into level $v$
$Q_r^v(T)$	rotational partition function for vibrational level $v$
$R_0, R_L$	mirror reflectivities
$t$	time
$t_{1/2}$	time to emit first 1/2 of the total pulse energy
$t_1$	pulse duration
$T$	temperature
$T_i$	initial temperature of the reacting mixture
$v$	vibrational quantum number
$\alpha_{th}$	threshold gain
$\alpha_{ri}, \beta_{ri}$	stoichiometric coefficients
$\alpha(v, J)$	optical gain for transitions to state $(v, J)$

$\eta$	laser efficiency
$\kappa_v$	rate of pumping into vibrational level $v$
$\nu_r$	reaction rate weighting factor
$\phi(v, J)$	Voigt profile for level $(v, J)$
$\psi_{ch}$	net chemical production rate ( $\text{mole}/\text{cm}^3\text{-sec}$ )
$\psi_{rad}(v, J)$	rate of stimulated emission from $(v + 1, J - 1)$ to $(v, J)$ , ( $\text{mole}/\text{cm}^3\text{-sec}$ )
$\omega_c(v, J)$	wave number for P-branch transitions into level $(v, J)$

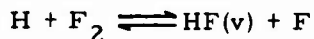
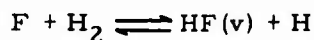
## I. INTRODUCTION

Increased interest in conversion of chemical energy into laser power and the scientific value of quantum-chemistry data available from the use of the chemical laser have stimulated recent experimental<sup>1-4</sup> and theoretical<sup>4-7</sup> studies. A current review of chemical laser technology has been made by Dzhidzhov, Platonenko, and Khokhlov.<sup>8</sup> The multiplicity of phenomena operating in a chemical laser makes quantitative predictions of laser performance or detailed interpretation of experimental data difficult without the aid of comprehensive modeling of these phenomena. Early modeling studies estimated the performance of a pulsed laser by considering the time history of gain on a given band, while the effect of the cavity and induced emission on the chemistry were neglected.<sup>6,7</sup> More recently, computer simulations have included these effects,<sup>4,9</sup> and such a code is used in this study. The simulation is used to study the effects of various parameters on the behavior of a pulsed HF laser. The principal objectives of this study are to determine:

1. Relative importance of the chemical kinetic mechanisms involved in the pulsed HF laser
2. Effect of the optical cavity on the reacting  $H_2 + F_2$  mixture
3. Effect of various parameters such as the initial concentrations and the initial temperature.

The method of simulation is similar to that used by Airey<sup>4</sup> for an HCl laser. The major provisions of the laser model are summarized as follows:

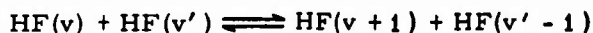
1. The dominant reactions used to represent the chemical processes in the reacting mixture are:
  - a. the  $H_2 - F_2$  chain



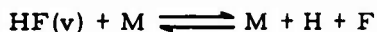
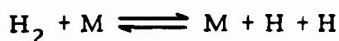
- b. vibrational-translational (VT) deactivation



- c. vibrational-vibrational (VV) quantum exchange



- d. dissociation-recombination



This reaction system is approximated by the 68 reactions listed in the Appendix.

2. The reacting mixture is homogeneous and is contained in a Fabry-Perot cavity.
3. For each vibrational level, the rotational levels have a Boltzmann distribution at the translational temperature.
4. Only one transition within a band can lase at a given time. This is the transition with maximum gain in the band and is always in the P-branch. During lasing on this line, the gain at line center is held constant at its threshold value.
5. Initiation is modeled by the instantaneous introduction of a finite concentration of F atoms into an initial gas mixture of  $\text{F}_2$ ,  $\text{H}_2$ , and Ar diluent, as might be caused by a very fast flashlamp or electrical discharge. A finite time history of  $\text{F}_2$  dissociation such as that produced by most initiation methods can be modeled and, indeed, might be of interest for modifying laser performance. Because of the additional parameters involved, such modeling was deemed outside the scope of the present study.

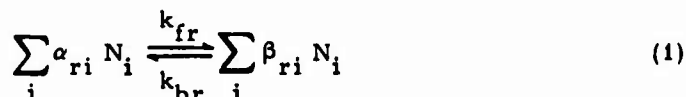
With similar assumptions and a simpler form of the reaction system, an analytical solution for a two-level model of a continuous chemical laser was obtained.<sup>5</sup> The present study extends that model to its multi-level equivalent and considers numerical solutions for a pulsed HF laser. The simulation is used to investigate the effect of the optical and chemical parameters on the laser's performance.



## II. THE CHEMICAL LASER COMPUTER SIMULATION

This section describes briefly the formulation of the chemical laser computer simulation. A detailed description is given in Ref. 9.

The chemical reactions may be written as



where  $N_i$  is the molar concentration of species  $i$ ,  $\alpha_{ri}$  and  $\beta_{ri}$  are stoichiometric coefficients, and  $k_{fr}$  and  $k_{br}$  are forward and backward rate coefficients. (The Nomenclature gives detailed definitions for symbols used in the text.)

The rate of change of concentration  $N(v)$  for vibrational level  $v$  is given by

$$\frac{dN(v)}{dt} = \psi_{ch}(v) + \psi_{rad}(v, J) - \psi_{rad}(v-1, J_L) \quad (2)$$

where the  $\psi_{rad}$  terms are rates of concentration change resulting from lasing into and out of level  $v$ . Lower level rotational quantum numbers  $J$  and  $J_L$  are selected as those giving maximum gain for transitions  $v+1 \rightarrow v$  and  $v \rightarrow v-1$ , respectively. Chemical reactions cause a rate of change  $\psi_{ch}(v)$  which is

$$\psi_{ch}(v) = \sum_r (\beta_{ri} - \alpha_{ri})(L_{fr} - L_{br}) \quad (3)$$

where

$$L_{fr} = k_{fr} \prod_j N_j \alpha_{rj}$$

*Preceding page blank*

and

$$L_{br} = k_{br} \prod_j N_j \beta_{rj}$$

The laser cavity is assumed to have a uniform photon flux with active medium length  $L$  and mirror reflectivities  $R_0$  and  $R_L$ . Lasing initiates for any  $v + 1 \rightarrow v$  band when the gain  $\alpha$  for the highest gain transition of that band is equal to the threshold gain  $\alpha_{th}$ , where

$$\alpha_{th} = -\frac{1}{2L} \ln(R_0 R_L) \quad (4)$$

The gain is assumed to be constant over length  $L$ . Only P-branch transitions need be considered; thus, the gain is given by Ref. 9

$$\alpha(v, J) = \frac{hN_A}{4\pi} \omega_c(v, J) \phi(v, J) B(v, J) \left[ \frac{2J+1}{2J-1} N(v+1, J-1) - N(v, J) \right] \quad (5)$$

where  $v$  and  $J$  refer to the lower level of the transition. The wave number of the transition is  $\omega_c(v, J)$ , and  $B(v, J)$  is the Einstein isotropic absorption coefficient based on the intensity. Line-broadening constants and resonance constants used in the Voigt profile at line center  $\phi(v, J)$  are those of Ref. 9.

A Boltzmann distribution at the translational temperature is taken for the rotational populations, hence

$$N(v, J) = N(v) \frac{(2J+1)}{Q_r^v(T)} e^{-hcE_J^v/kT} \quad (6)$$

where values of rotational partition function  $Q_r^v(T)$  and rotational energy  $E_J^v$  are from data of Mann, et al.<sup>10</sup>

The energy equation for a constant density gas is written in the form

$$\sum N_i C_{pi} \frac{dT}{dt} - \frac{dp}{dt} = - P_L - \sum \frac{dN_i}{dt} H_i \quad (7)$$

where  $C_{pi}$  is the specific heat at constant pressure and  $H_i$  the molar enthalpy of species  $i$ ,  $p$  is the pressure, and  $P_L$  is the output lasing power per unit volume. This power is given by

$$P_L(t) = \sum_{v=0}^5 h c N_A \omega_c(v, J) \psi_{rad}(v, J) \quad (8)$$

and the pulse energy released in time  $t$  is

$$E_L(t) = \int_0^t P_L(t') dt' \quad (9)$$

Chemistry and thermodynamics determine the production of excited species until, at some time  $t_0$  and for some  $J = J_0$ , the gain on a given vibration-rotation transition reaches  $\alpha_{th}$ . At this time, the laser pulse begins. Then Eqs. (2), (4), and (7), along with the state equation, are solved for the temperature, pressure, concentrations, and the  $J$  for each band that is lasing as a function of time. During lasing, the value of  $J$  may change; this process will be referred to as a "J-shift." Lasing terminates when all gains drop below  $\alpha_{th}$ .

### III. MECHANISMS OF THE PULSED HF LASER

#### A. GENERAL ENERGY INTERPRETATION

The initial gas mixture in the laser cavity has a given concentration ratio  $F_2:H_2:F:Ar$ , where the F atoms represent varying degrees of  $F_2$  dissociation by some initiation scheme. The diluent Ar is used mainly for temperature control. A typical time history of the total pulse power is shown in Fig. 1, and curves depicting rate of laser energy release for the bands lasing are shown in Fig. 2(a). For this case, the initial  $F_2:H_2:F:Ar$  is 1:1:0.1:50, where one unit of concentration is equivalent to  $9.4072 \times 10^{-7}$  mole/cc. This unit is used throughout this work. Initial temperature and pressure are 300° K and 1.207 atm, respectively. Mirror reflectivities are 0.8 and 1.0, and the active medium length is 100 cm. This case serves as a standard, and excursions from it comprise the parametric study.

In the course of the reaction, the temperature and the concentrations of HF(v) increase, causing the J value for maximum gain on a given vibrational band to increase. In the calculation when lasing shifts to the next higher J, there is a discontinuous, but small, increase in the rate of photon emission. In Fig. 2(b), the laser energy emission rate for the 2-1 band is shown as a function of time with all the J-shift details included. The J's used to label J-shifts on the 2-1 band are associated with the  $v=1$  level. The discontinuities without labels are caused by J-shifts on adjacent bands. For simplicity, discontinuities have been smoothed in Figs. 1 and 2(a).

The following paragraphs give an interpretation of the major mechanisms of the standard case. The initial emission "spike" results from the pumping of HF(v) levels by Reaction 8-10.<sup>11</sup> During this spike, approximately 80% of the initial F-atom concentration is consumed (Fig. 3). The increase in the rate of photon emission after the initial spike is due to an increase in temperature and to the increasing importance of Reactions 14-20 as a result of the production of H by Reactions 7-10 and, hence, the operation of the chain.

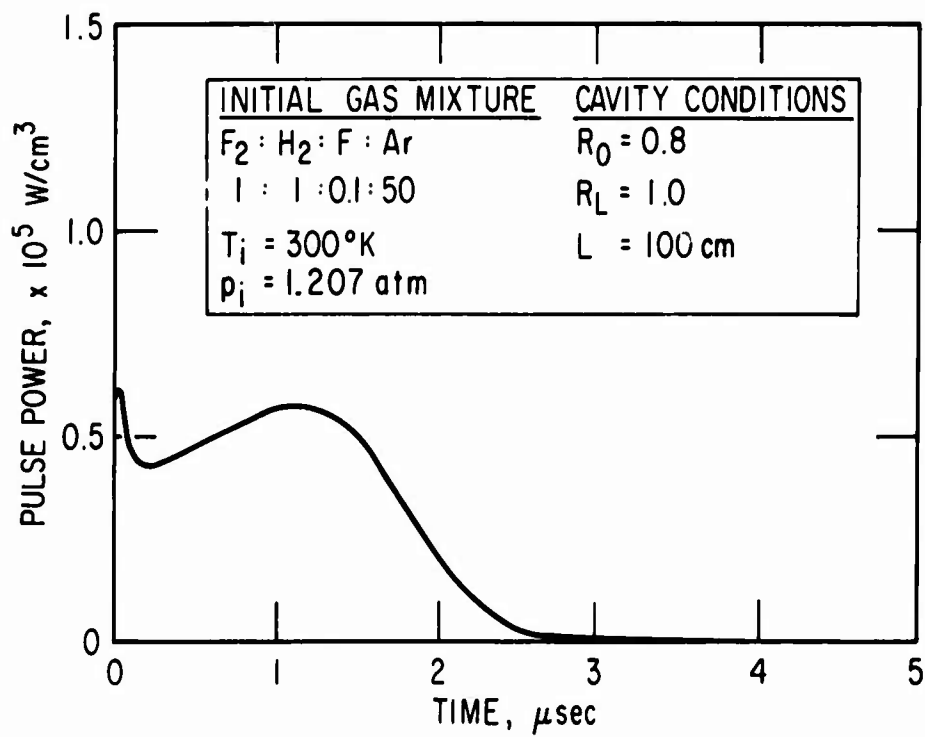
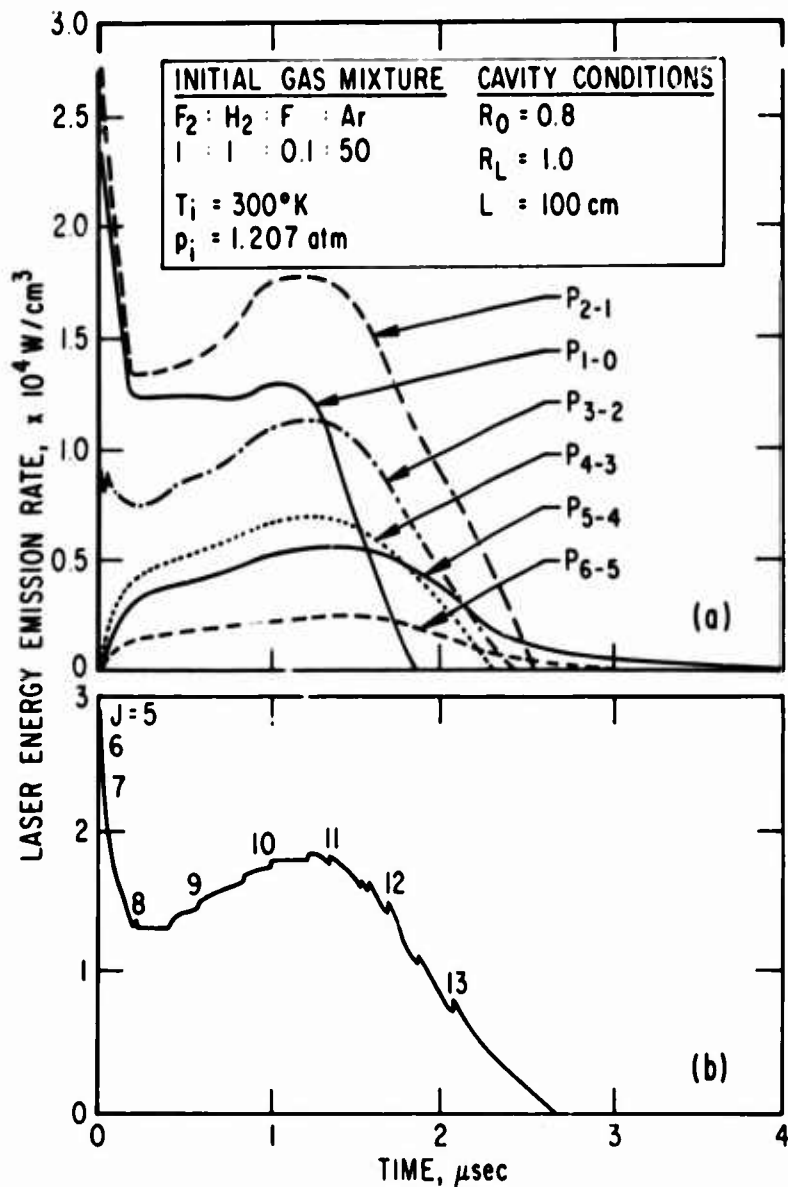


Figure 1. Power History of the Standard Case



**Figure 2. Laser Power and Energy Emission Rate**

(a) Laser power from the first six levels of HF. (b) Laser energy emission rate from the 2-1 band for the standard case. The new value of  $J$  for the lower level is shown for each  $J$ -shift location.

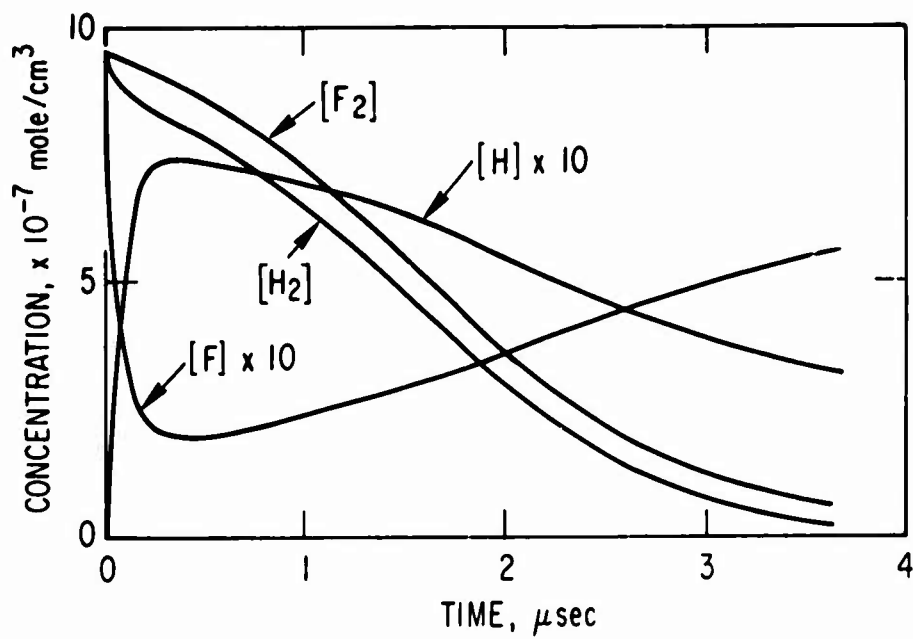


Figure 3. Time Histories of the Concentrations of  $H_2$ ,  $F_2$ ,  $H$ , and  $F$  for the Standard Case

Termination of the lasing pulse is caused in part by the depletion of the  $H_2$  and  $F_2$  (Fig. 3). In addition, as the fuel supply is consumed, the pumping rate decreases until chemical deactivation of  $HF(v)$  forces the gain below threshold.

The set of equations (2) may be solved for emission on a particular band  $\psi_{rad}(v, J)$  and then put in the form

$$\sum_{v'=v+1}^6 \kappa_{v'} = \psi_{rad}(v, J) + \sum_{v'=v+1}^6 \frac{dHF(v')}{dt} + D_{v+1, v} \quad (10)$$

where  $\kappa_{v'}$  is the rate of pumping into level  $v'$  by the Reactions 8-10 and 15-20, and  $D_{v+1, v}$  is the chemical deactivation rate of the  $v+1, v$  inversion. In general, the VV HF-HF deactivation reactions are not very important when compared to VT deactivation; hence, the major contribution to  $D_{v+1, v}$  is deactivation of  $HF(v+1)$  by VT reactions and VV reactions with  $H_2(v')$ . In fact, these are the only contributions to  $D_{v+1, v}$  when anharmonic effects are negligible. Of course, Eq. (10) is a result of conservation of number density of  $HF(v)$ , and terms in the equation may be interpreted as

$$\left[ \begin{array}{c} \text{Pumping} \\ \text{Rate} \end{array} \right] = \left[ \begin{array}{c} \text{Photon} \\ \text{Emission} \\ \text{Rate} \end{array} \right] + \left[ \begin{array}{c} \text{Level} \\ \text{Filling} \\ \text{Rate} \end{array} \right] + \left[ \begin{array}{c} \text{Chemical} \\ \text{Deactivation} \\ \text{Rate} \end{array} \right]$$

where level filling is the filling of vibrational levels as needed to maintain the required gain. The relative sizes of the terms in Eq. (10) for the 2-1 band are shown in Fig. 4, where the rate of photon emission on that band is also shown as a solid line. Note that Eq. (10) is essentially a representation of the distribution of pumping energy when anharmonic effects are small.

Distribution of the pumping rates among the vibrational levels has a significant effect on the energy available for lasing. For example, the production of one  $HF(6)$  molecule makes up to six times more energy available for lasing than the production of one  $HF(1)$  molecule. Pumping reactions



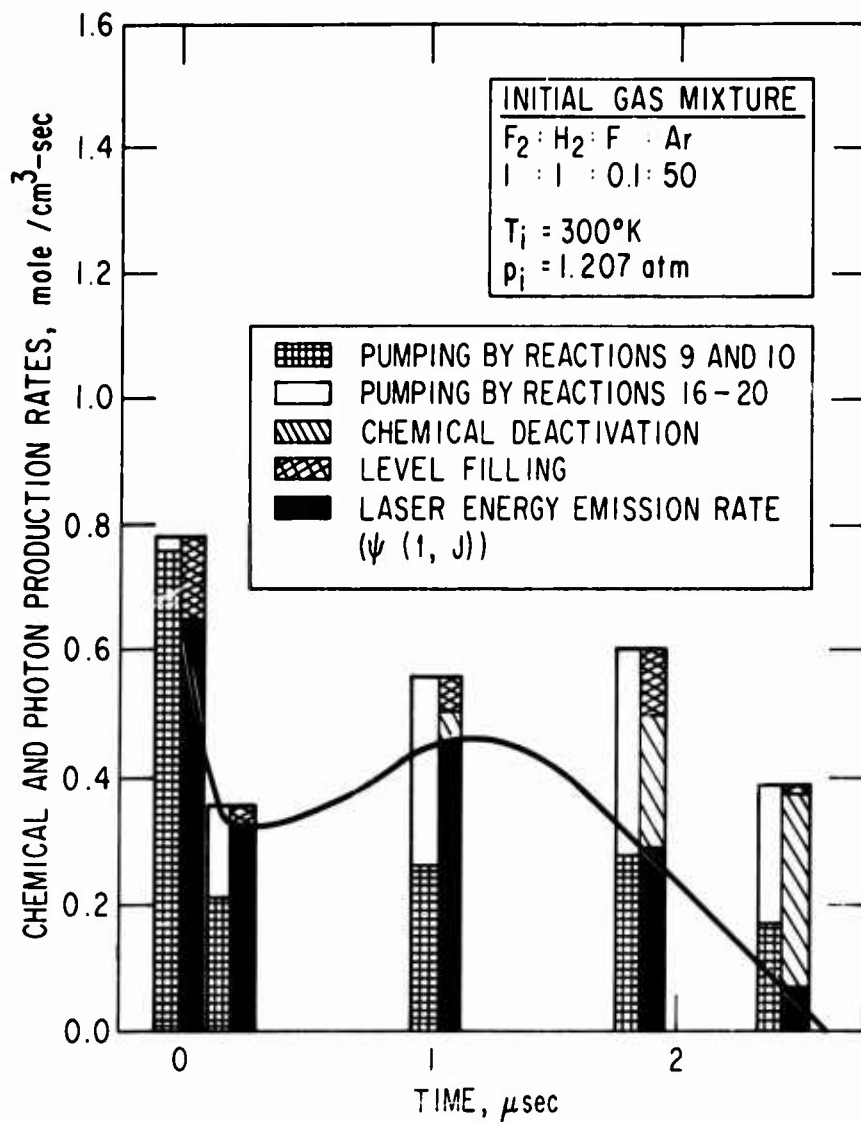


Figure 4. Relationship of Dominant Mechanisms for the 2-1 Band of HF in a Chemical Laser

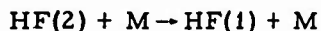
The solid curve represents the instantaneous rate of release of lasing photons for the 2-1 band

such as 8 and 9 that promote a total inversion are more favorable for meeting threshold conditions than the more even pumping distribution of Reactions 15-20. In regimes where threshold is easily attained and in the absence of deactivation, changes that increase the pumping of Reactions 15-20 relative to Reactions 8-10, such as H or F<sub>2</sub> rich mixtures, can be expected to increase pulse energy, since they supply more vibrational energy per mole of fuel.

#### B. A DETAILED INTERPRETATION OF MECHANISMS FOR THE STANDARD CASE

This section describes in detail the mechanisms that promote the partial inversion and contribute to laser power from the 2-1 band. In addition, we shall assess the effect of the photon flux on the chemical mechanisms associated with this band.

The concentration difference HF(2)-HF(1) is nearly proportional to the gain on the 2-1 line, Eq. (5). The relative importance of the chemical reactions and photon emissions that alter the  $v = 2$  to  $v = 1$  inversion is depicted in Fig. 5(a). The rate of mass transport by a given reaction is  $L_{fr} - L_{br}$ . A weighting factor  $\nu_r$  is used to give the appropriate contribution of each reaction to the increase of HF(2)-HF(1). For example, the VT reaction



decreases HF(2) and increases HF(1). The effective mass transported is twice ( $L_{fr} - L_{br}$ ) for the reaction; hence,  $\nu_r = 2$ . The major contribution to mass transport during the initial stages of the reaction results from lasing on the 2-1 and adjacent bands. At  $t = 0$ , only the pumping Reactions 8 and 9 are present. In the figure, the first bar shown is for  $t = 0+$ . The initial spike in the photon emission rate is a result of the high initial F concentration, and the remainder of the curve (Fig. 1) may be interpreted by noting the effect of temperature rise and action of the chain, as will be shown later.

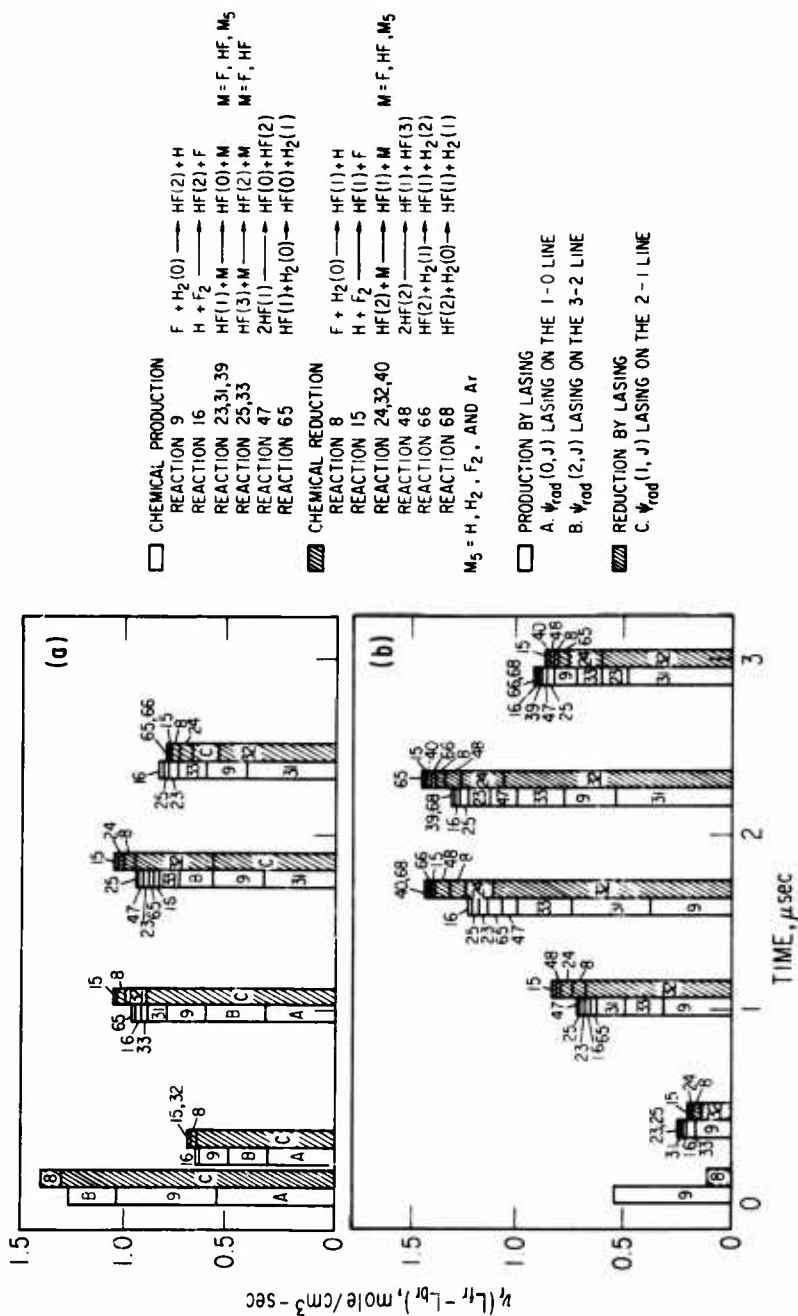
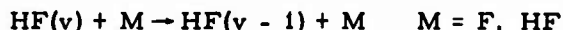


Figure 5. Production and Reduction Mechanisms for the Gain of the 2-1 Line  
 (a) Standard case. (b) Standard case with radiation suppressed.

In the preceding section, the significance of pumping by Reactions 16-20 was noted. The format of Fig. 5(a) tends to mask this significance, for at first glance Reactions 8 and 9 appear to be the dominant chemical pumping mechanisms. However, Reactions 16-20 pump the upper vibrational levels and contribute to the pumping of  $v=2$  by cascading. We note that the major pumping and deactivation of the 2-1 inversion arises from lasing on the bands 1-0, 2-1, and 3-2. Lasing terminates before the fuel supply ( $F_2$  and  $H_2$ ) is consumed because the VT chemical deactivation



becomes large enough to force the gain below threshold. The rate of mass transport by all other reactions is small.

We examine the standard case with radiation suppressed by operating the code with reflectivities set equal to zero. Production and reduction mechanisms of the 2-1 inversion for this zero-power case are shown in Fig. 5(b). Comparing Figs. 5(a) and 5(b), we note that in the absence of a photon flux both pumping of the  $HF(v)$  levels and their deactivation rates are larger. Pumping is larger because the gas is hotter (hence, the reactions are faster), as is shown in Fig. 6, where the temperature history of the standard case and the zero-power calculations are compared. The increase in deactivation is caused by the presence of higher concentrations of  $HF(v)$ . The higher populations in the  $HF(v)$  levels for the zero-power case also result in an increased significance of VV reactions (47, 48, 65, 66, and 68) of  $HF(v)$  with  $HF(v')$  and  $H_2(v'')$ . In addition, we see in Fig. 5(b) that VT deactivation of  $HF(v)$  by the diluent (Reactions 39 and 40) begins to appear.

For the lasing case, the gain reaches threshold and remains at that value, but in a zero-power calculation the maximum gains for the lower transitions reach values nearly 3 orders of magnitude larger than the threshold value (Fig. 7). In the figure, locations where the gain for a given band becomes larger for a new value of  $J$  are denoted by the new  $J$ . A comparison of the gain on the 4-3 band in Fig. 7 with the 4-3 curve in Fig. 2(a) shows the

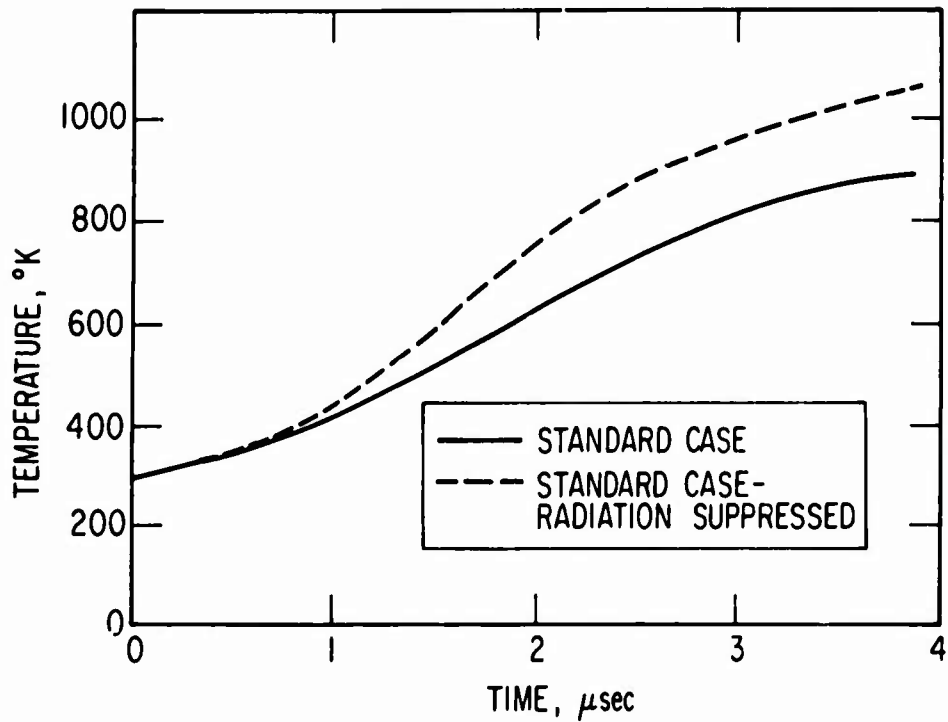


Figure 6. Temperature History of the Standard Case, with and without Radiation Suppressed

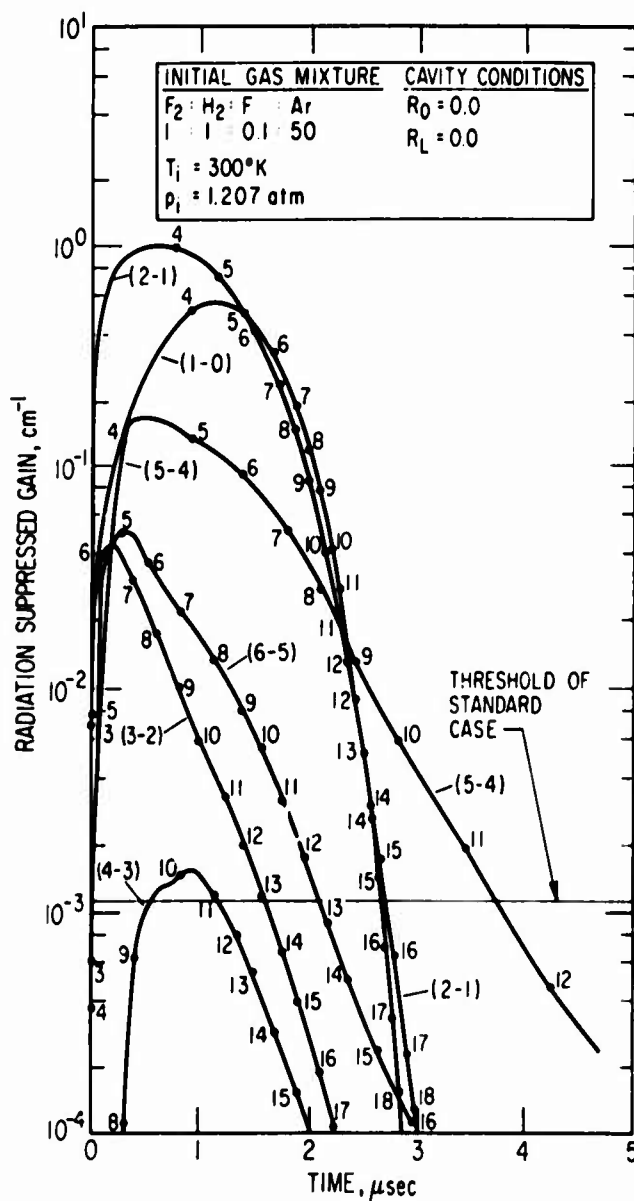


Figure 7. Gain History for Standard Case with Radiation Suppressed

importance of radiative cascading and the limited usefulness of zero-power gain calculations for a multi-level system such as this.

In Fig. 8, production and reduction mechanisms for the F-atom population are shown. After a transient period of consumption of F atoms by Reactions 7-10, the production and reduction mechanisms are nearly the same, which illustrates the presence of a quasi-steady chain.

As indicated earlier, the second hump in the laser photon emission curve may be explained by noting the effect of the temperature increase. Rate coefficients characteristic of the important chemical mechanisms are depicted as a function of time for the standard case in Fig. 9. The pumping rates increase, while the principal deactivation rate decreases with time. Hence, temperature variations of rate coefficients during the pulse tend to increase the instantaneous rate of photon emission and reduce chemical deactivation losses. At still higher temperatures, the VT deactivation rate of HF begins to increase with temperature, as is illustrated for Reaction 32 in the insert in Fig. 9. The increase in the photon emission curve (Fig. 2) between 0.15 and 1.0  $\mu$ sec may be attributed to an increase in pumping with the rise in temperature. This may be seen by comparing Fig. 9 with Fig. 3. During this time interval, the reactant concentrations decrease slightly, whereas, due to the temperature rise, the pumping reaction rates increase by a factor of 2.

From the previous discussion, it is clear that the important rate coefficients give a more favorable competition between stimulated emission and deactivation with a temperature somewhat above 300° K. With pumping increased relative to deactivation, the pulse energy is larger because more of the fuel is consumed while the reacting mixture is above threshold. The effect of a temperature increase on the pulse duration is less certain. While the overall reaction is faster, the increased pumping relative to deactivation tends to hold the mixture above threshold for a longer time.

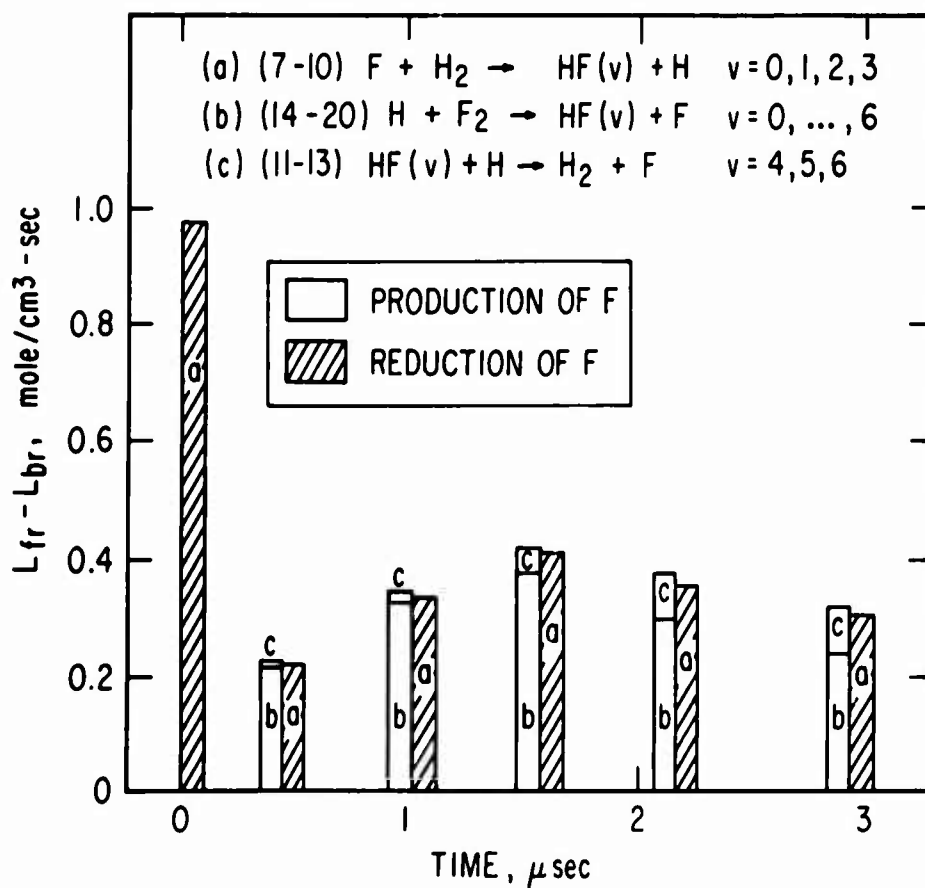


Figure 8. Mechanisms Producing and Reducing F-atom Concentration for the Standard Case



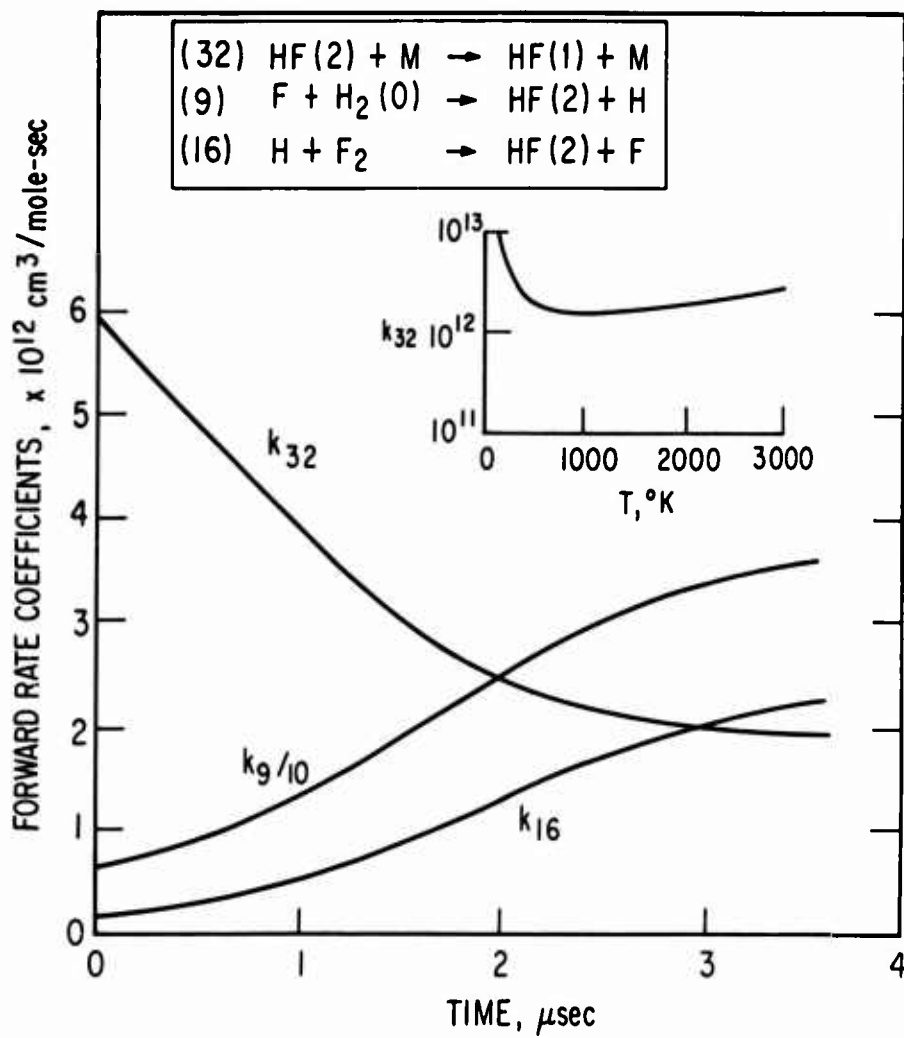


Figure 9. Time Histories of Important Rate Coefficients for the Standard Case

#### IV. PARAMETRIC VARIATION

The laser pulse may be characterized in part by the pulse duration  $t_1$  and total pulse energy  $E_L(t_1)$ . In the parametric study, we encounter many pulses with long low-power tails; hence, the time  $t_{1/2}$  required to release one-half the pulse energy  $E_L(t_1)/2$  is also a useful characteristic. The effect of varying the initial chemical concentrations, cavity conditions, and rate coefficients is discussed by interpreting the variations in these pulse characteristics.

##### A. THRESHOLD

Concentrations and temperature are given the same initial values as in the standard case, while the characteristics of the optical cavity (mirror reflectivities and cavity length) are varied. This is equivalent to varying  $\alpha_{th}$ , as can be seen from Eq. (4). In Fig. 10, the variation of pulse energy with  $\alpha_{th}$  is shown. Additional abscissa scales for equivalent values of  $R_0$  and  $L$  are also shown. In Fig. 10, the pulse energy is zero for  $\alpha_{th} \geq 1.0$ . This is consistent with expectations based on the maximum gain shown in Fig. 7. As  $\alpha_{th}$  approaches zero, the pulse energy approaches a maximum; of course, practical limitations on cavity losses and cavity length can make realization of this maximum difficult. One aspect of decreasing  $\alpha_{th}$  is that, in addition to increasing  $E_L(t_1)$ , the pulse length characterized by  $t_{1/2}$  or  $t_1$  is also extended, as shown in Fig. 11. For decreasing values of  $\alpha_{th}$ , the pronounced increase in  $t_1$  relative to  $t_{1/2}$  is the result of a long low-power tail. The time required for release of the majority of the pulse energy is relatively insensitive to  $\alpha_{th}$ , as seen by the small variation of  $t_{1/2}$ .

Since more energy is extracted for low  $\alpha_{th}$ , the temperature of the reacting mixture is also lower. As  $\alpha_{th}$  is decreased, the vibrational populations are smaller and the rate of VT chemical deactivation is reduced, even though the rate coefficients for these processes are higher because of the lower temperature. Examination of the reaction rates for the 2-1 band shows that for smaller values of  $\alpha_{th}$  the rate of pumping is larger, the instantaneous

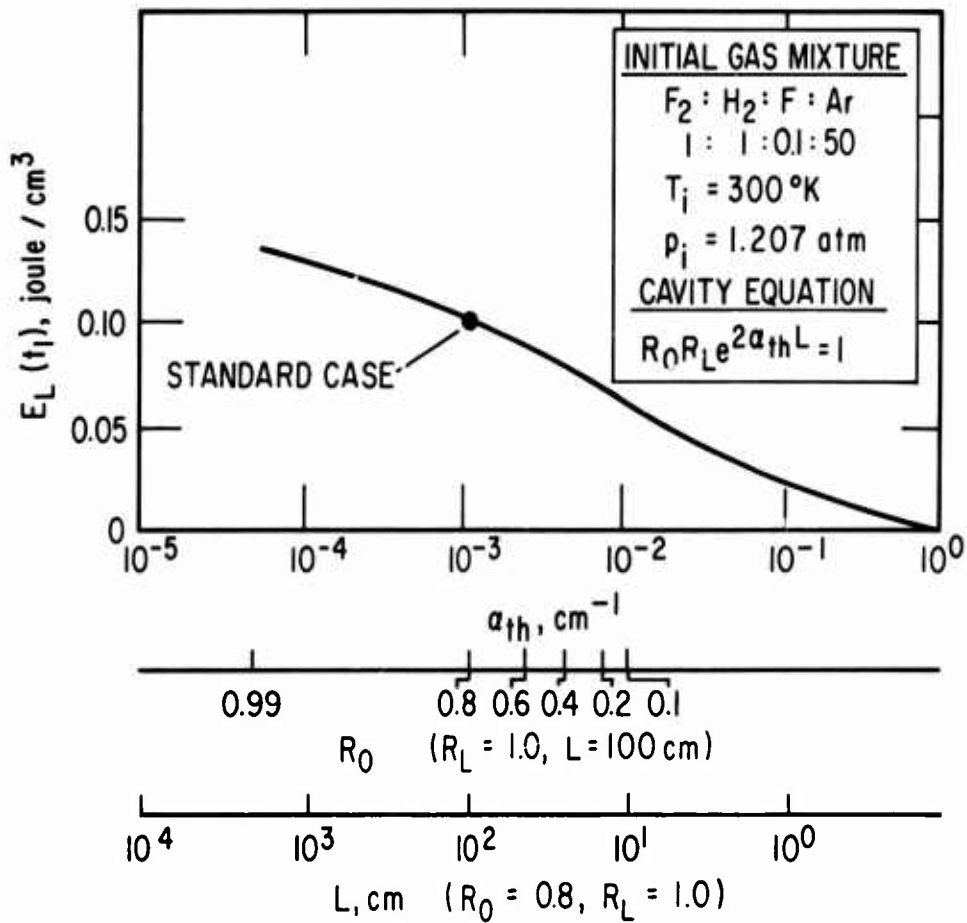


Figure 10. Effect of Threshold Gain on Pulse Energy

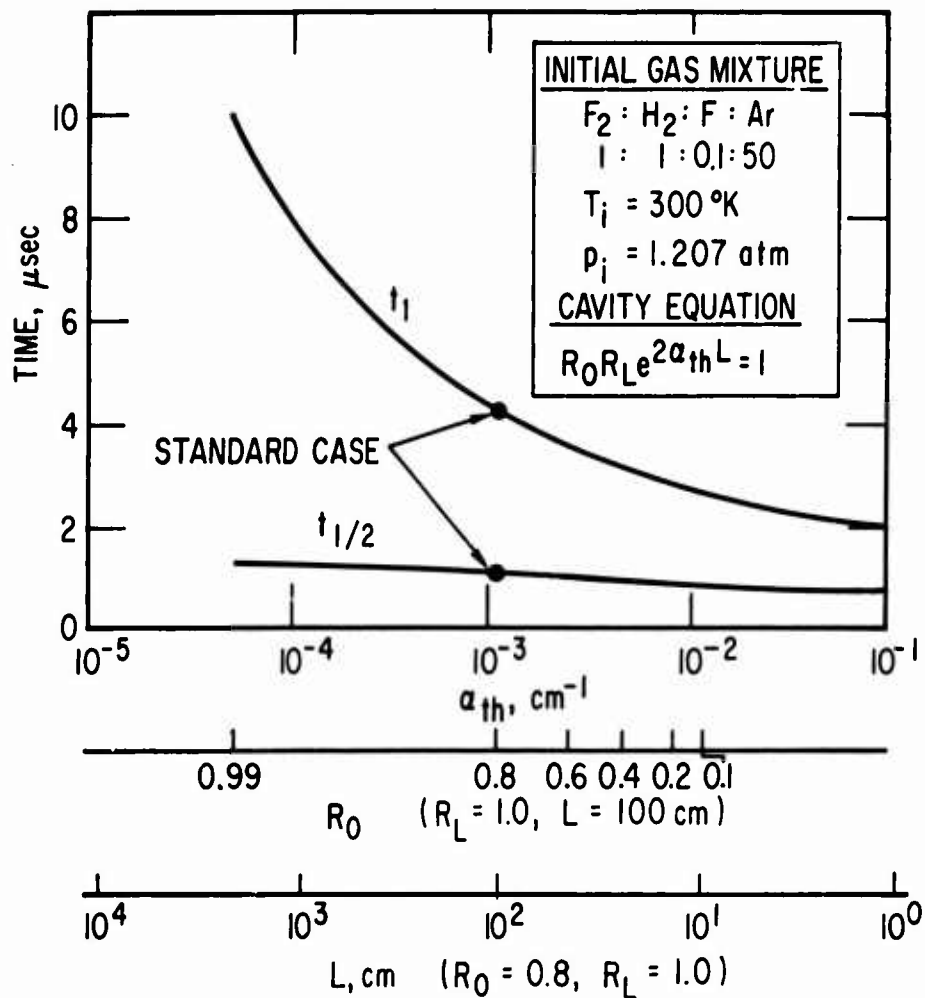


Figure 11. Effect of Threshold Gain on  $t_1$  and  $t_{1/2}$

power is larger, and the rate of level filling (energy storage) becomes smaller. The mixture reaches threshold at an earlier time and, thus, the F-atom concentration is larger, and pumping at pulse initiation is higher and continues to be so throughout the run.

#### B. DILUENTS

Diluents contribute to the heat capacity of the total system and act as catalysts for the VT deactivation reactions and recombination reactions. Since the VT deactivation rate of HF(v) with Ar is about  $10^5$  times smaller at 300°K than the VT rate of HF(v) with itself, Ar contributes little to chemical deactivation; its major role is temperature control.

The effect of variations in dilution is studied for two initial concentrations of F. For initial F equal to 10% of initial  $F_2$ , the following trends are noted as the concentration of Ar is increased.

1. The temperature rise throughout the reaction is less, as expected.
2. The laser power decreases and the second peak in the power curve disappears. Also, pumping and level filling rates decrease while deactivation rates increase as a result of the lower temperature.
3. The pulse energy decreases gradually (Fig. 12) because of the less favorable competition described in Item 2.
4. The pulse duration  $t_1$  and time parameter  $t_{1/2}$  increase, as expected, for lower temperatures (Fig. 13).

Initial F concentrations in this 10% range and above emphasize Reactions 8-10 relative to Reactions 15-20.

For initial F equal to 1% of initial  $F_2$ , pumping rates throughout the reaction are much lower. Deactivation is more significant and the pulse energy is lower. As the concentration of Ar is increased, the temperature throughout the pulse is lower and the pulse length is increased. Further

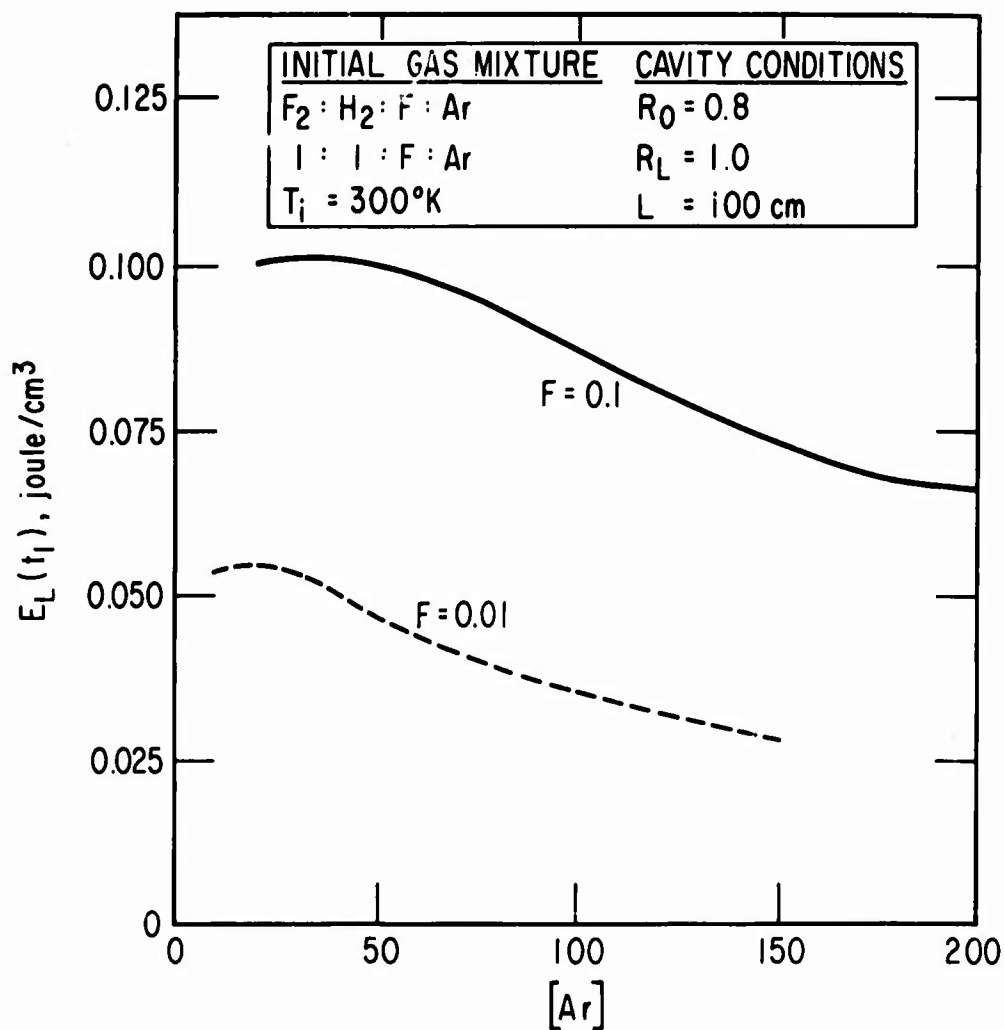


Figure 12. Effect of Diluent Concentration on Pulse Energy with Two Different Initial F-atom Concentrations

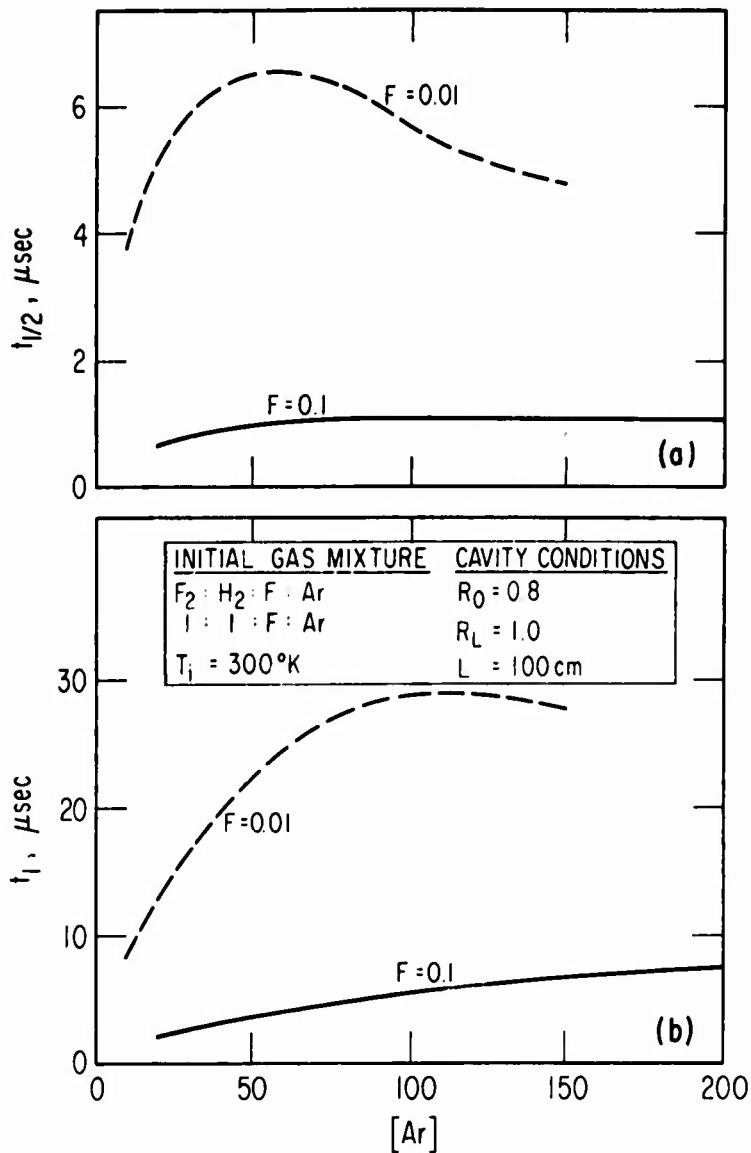


Figure 13. Effect of Diluent Concentration on  $t_{1/2}$  and  $t_1$   
 (a) Effect on  $t_{1/2}$  with two initial F-atom concentrations. (b) Effect on pulse length  $t_1$  with two initial F-atom concentrations.

increases in Ar lower the temperature sufficiently such that the stimulated emission-deactivation competition forces the pulse length to decrease and a maximum pulse duration is found.

### C. INITIAL F<sub>2</sub> DISSOCIATION

The initial F-atom concentration is increased while the stoichiometric balance is maintained between hydrogen and fluorine. Other initial conditions are held constant. As the concentration of F is increased from very low values, the following trends are noted.

1. The rate of pumping increases, laser power increases, and the rate of level filling increases.
2. The faster pumping rates result in smaller pulse durations  $t_1$  and smaller values of  $t_{1/2}$  (Fig. 14).
3. The pulse energy increases until the mass fraction of F reaches 0.2 (Fig. 15). Further increases in F result in a dominance of reactions 7-10 throughout the pulse. The second peak in the power curve disappears, and  $E_L(t_1)$  and  $E_{v+1,v}$  for each band decrease. Finally, for total dissociation of F<sub>2</sub>, Reactions 14-20 do not contribute to the pulse energy and  $E_{43}$ ,  $E_{54}$ , and  $E_{65}$  are zero.
4. Since the pumping Reactions 7-10 release only about one-third as much energy as Reactions 14-20, the reaction temperature is lower for large initial F. Such behavior leads to the stimulated emission-deactivation competition suggested in the discussion of the standard case.
5. For small concentrations of F, there is a strong competition between stimulated emission and deactivation. As initial F<sub>2</sub> dissociation increases, the relative importance of VT deactivation decreases until Reactions 23-30 make a significant contribution.



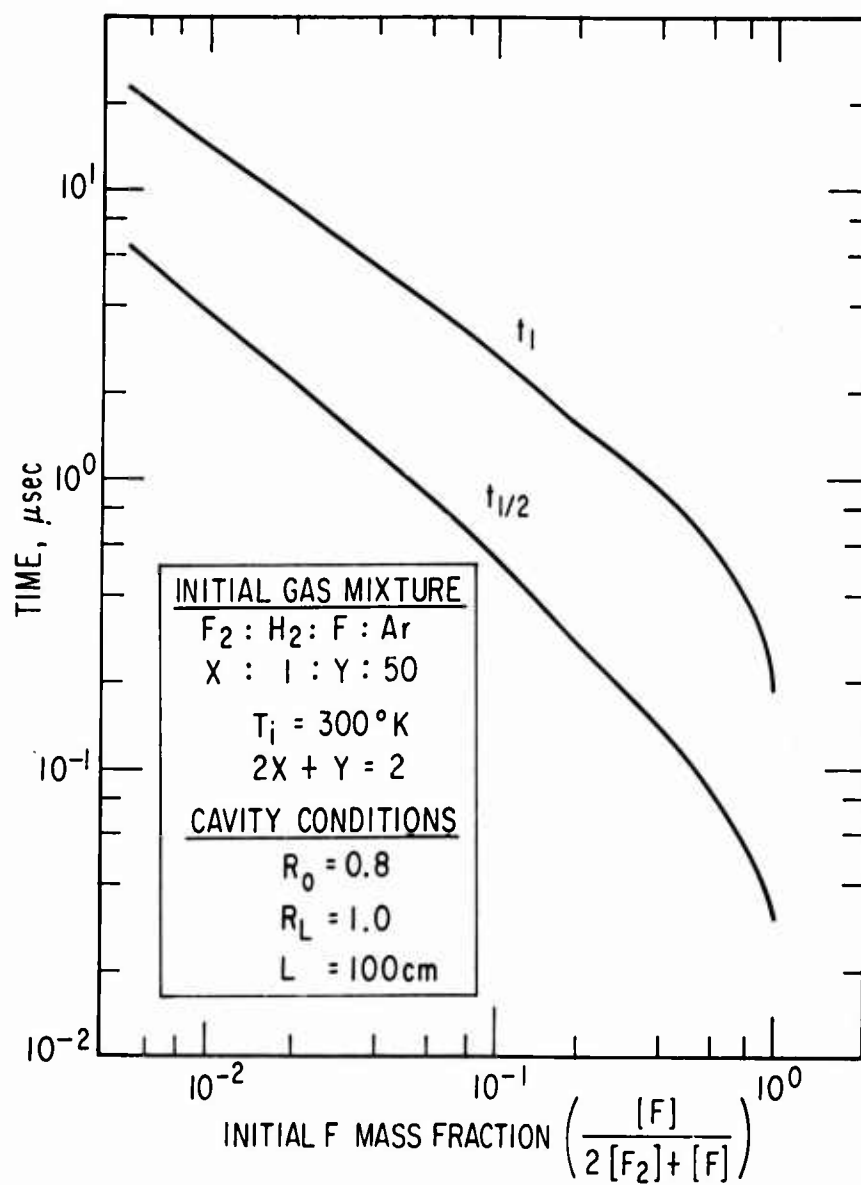


Figure 14. Effect of Initial  $\text{F}_2$  Dissociation on Pulse Length

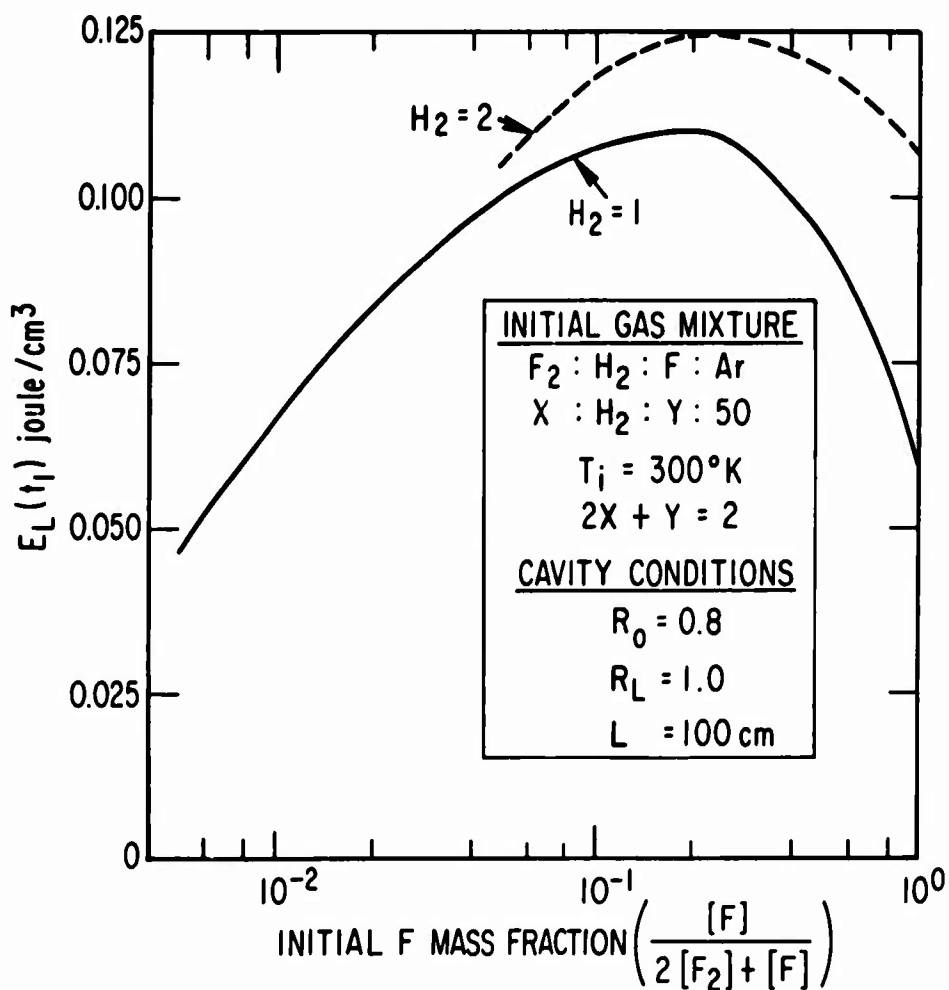


Figure 15. Effect of Initial  $F_2$  Dissociation on Pulse Energy

For the larger initial F concentrations, the mixture is below stoichiometric for  $H_2$ . To assess this effect, the same variations of F were made with the initial  $H_2$  concentration doubled. The results of these computations are shown in Fig. 15 as a dashed curve. There is a marked increase in pulse energy for high initial F. There is also a slight decrease in  $t_1$  and  $t_{1/2}$  as a result of the increased reaction rates.

#### D. INITIAL TEMPERATURE

The initial temperature  $T_i$  was varied while all other conditions were maintained at the values of the standard case. As  $T_i$  increases, the temperature throughout the pulse is higher, reaction rates are faster, and characteristic times become shorter (Fig. 16). For  $T_i$  above 400°K, the hump in the power curve disappears; i.e., throughout the pulse the rate of pumping decreases monotonically, since the effect of temperature increase is less significant. In addition, the pulse energy begins to decrease slightly; however, the overall effect of  $T_i$  on pulse energy is small.

#### E. INITIAL $H_2$ CONCENTRATION

The initial concentration of  $H_2$  is varied while other initial conditions are those of the standard case. The pulse energy and pulse duration are both quite sensitive to the initial  $H_2$  concentration for  $H_2$ -lean mixtures (Fig. 17). In this regime, increases in  $H_2$  are accompanied by increased pumping, increased pulse energy, and increased pulse duration.

The effect of variations in  $H_2$  is very small for  $H_2$ -rich mixtures. As the  $H_2$  concentration is increased, the pumping rate increases, the pulse energy increases, and the pulse duration decreases because of the faster reaction rate. Note that the time  $t_{1/2}$  required to deliver one-half the pulse energy is virtually independent of initial  $H_2$ . Of course, very high  $H_2$  concentrations give rise to VV and VT deactivation of  $HF(v)$  with  $H_2(v')$ .

#### F. VARIATION OF IMPORTANT RATE CONSTANTS

The effect of variations in dominant rate constants was studied with variations from the standard (see Appendix) selected to include the major

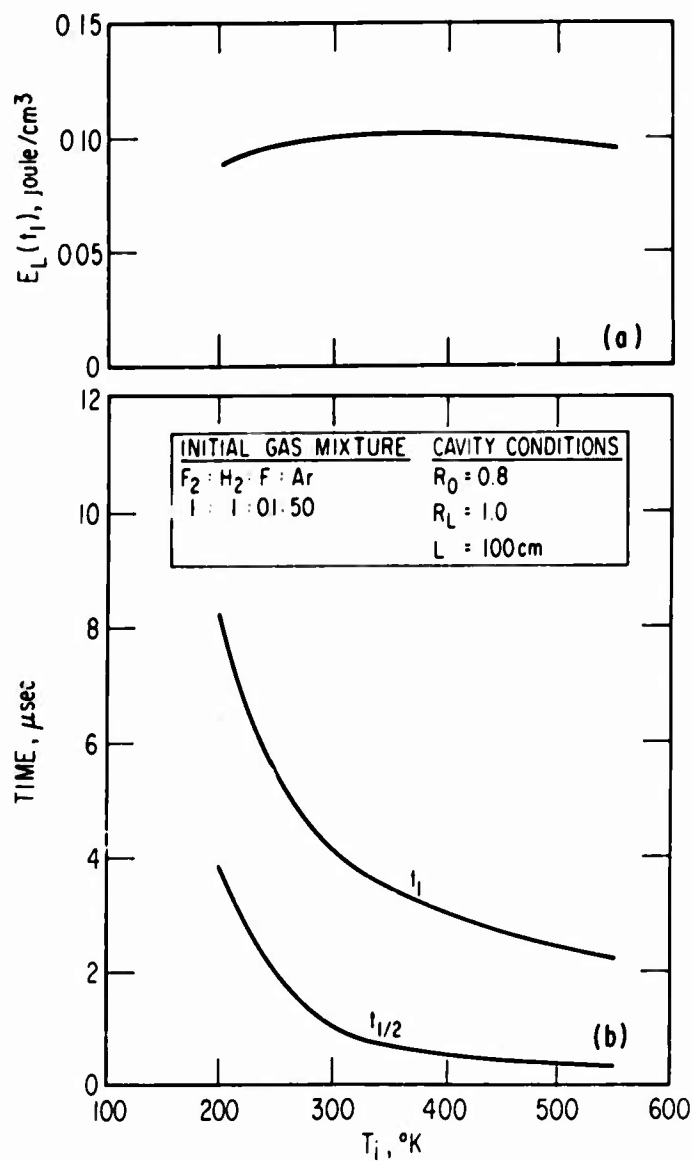


Figure 16. Effect of Initial Temperature

(a) Effect on pulse energy. (b) Effect on  $t_1$  and  $t_{1/2}$

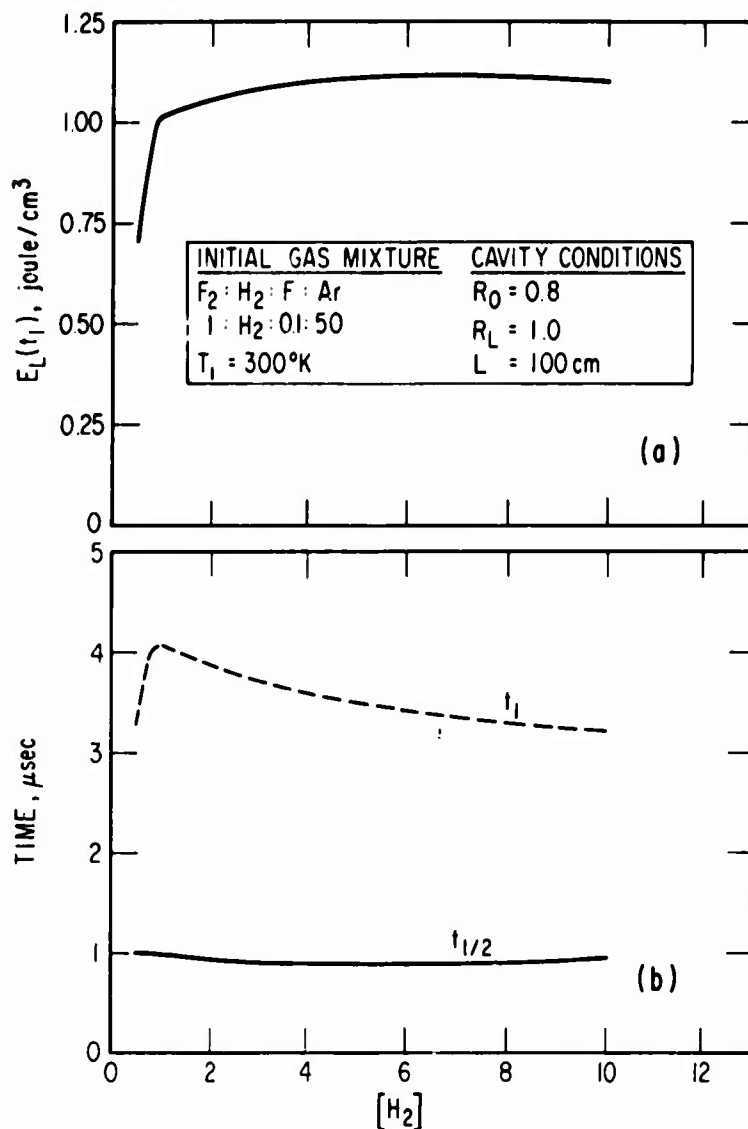


Figure 17. Effect of Initial  $H_2$  Concentration

(a) Effect on  $E_L(t_1)$ . (b) Effect on the characteristic times  $t_1$  and  $t_{1/2}$ .

uncertainties in the rates at the time of the study. The effect of these changes on the pulse characteristics and the energy released from the band  $v + 1 \rightarrow v$ ,  $E_{v+1,v}$ , may be seen in Table I. The variations in the rates studied are described below.

Rate 1: Pumping into vibrational levels 1-6 is reduced by a factor of 2, while the total reaction rate is held constant by increasing the rate of production of HF(0). As expected, the pulse energy and the pulse length decreased with the lower pumping. Also, the energy in the 1-0 band is much less because the rate of populating HF(0) is much higher.

Rate 2: The rates for HF-HF VV reactions are increased by a factor of 100. This change has a very small effect on the pulse energy and the characteristic times; however, it does redistribute the energy emitted by the various bands.

Rate 3: The rates for HF-H<sub>2</sub> VV reactions are increased by a factor of 100. In this case, the pulse energy is essentially constant, the energy in the 2-1 band is higher while the energy in the 1-0 band is lower. Reaction 65 becomes a significant deactivation mechanism for the 1-0 inversion, and for this mixture the combination of Reactions 65 and 66 aids the 2-1 inversion. In addition, since the 1-0 band contributes energy early in the pulse,  $t_{1/2}$  increases slightly.

Rate 4: The changes in Rates 1, 2, and 3 are combined. A much lower pulse energy and shorter pulse duration are observed, as expected.

Rate 5: The backward rates for  $F + H_2 \rightleftharpoons HF(v) + H$ ,  $v = 4, 5, 6$  are reduced by a factor of 100. The pulse energy increases 10%. A marked increase in the energy released in the bands 6-5, 5-4, and 4-3 is noted as a result of the rate change, and the energy released in the lower bands is higher as a result of cascading.

Table I. Effect of Rate Changes on Pulse Characteristics

Rate	Energy, joule/cc							Time, $\mu$ sec	
	$\underline{E}_{10}$	$\underline{E}_{21}$	$\underline{E}_{32}$	$\underline{E}_{43}$	$\underline{E}_{54}$	$\underline{E}_{65}$	$\underline{E}_L(t_1)$	$\underline{t}_1$	$\underline{t}_{1/2}$
Standard									
1-Low pumping	.0208	.0337	.0195	.0115	.0109	.0048	.101	4.09	1.0
2-High VV-HF	.0028	.0115	.0069	.0038	.0044	.0019	.0313	2.86	0.7
3-High VV-H <sub>2</sub> *	.0151	.0400	.0235	.0123	.0112	.0049	.107	3.96	1.0
4-Combination of 1, 2, and 3	.0177	.0347	.0193	.0114	>.0109	.0048	.0988	>3.7	1.1
5-Reduced backward cold reaction	.0003	.0109	.0082	.0041	.0043	.0019	.0297	2.83	0.8
	.0213	.0347	.0221	.0153	.0124	.0053	.111	3.57	1.1

\* This computation was extremely long and the 5-4 band was still lasing at a very low level at termination of the run.

## V. CHEMICAL EFFICIENCY

Of the 31.56 kcal/mole released by Reactions 7-10, 22.6 kcal/mole is supplied as vibrational energy of HF(v) with the pumping rates listed in the Appendix. Reactions 14-20 release 98.04 kcal/mole of which 43.1 kcal of vibrational energy is available. By combining these reactions, we find 50.7% of the chemical energy converted to vibrational energy. After the threshold condition and chemical deactivation are considered, only a fraction of this vibrational energy is available for laser emission.

A thermodynamic efficiency of the laser system would account for the energy required to dissociate  $F_2$  upon pulse initiation. However, for simplicity, efficiency  $\eta$  will be taken as

$$\eta = \frac{E_L(t_1) \times 100/\text{mole } F_2}{129.6 \text{ kcal/mole } F_2} \quad (11)$$

Thus, pumping rates alone require  $\eta$  to be less than 50.7% for the chain. For the standard case,  $\eta$  is 20.6%. Optimization of  $\eta$  has not been attempted. However, we note that the effects of the parameters studied in this report indicate the probable direction to be taken for optimization, and that the variation of  $\eta$  is approximately like that of  $E_L(t_1)$ .



## VI. SUMMARY AND CONCLUSIONS

A computer simulation is used to study the interaction of the chemistry and the optical cavity of a pulsed HF laser. A detailed study of the effect of the optical cavity, the initial chemical composition, the initial temperature, and variations in uncertain chemical rate coefficients on the pulse length and pulse energy is made. Variations about a standard case are used to study the effect of these parameters.

Pumping, vibrational-translational deactivation reactions, temperature control, and threshold gain are found to be important parameters governing the behavior of the laser. A competition between stimulated emission and deactivation is observed, and conditions where the effect of deactivation is minimized are indicated. A decrease in the threshold gain is accompanied by an increase in pulse energy and pulse duration. The photon flux is found to have a large effect on the populating mechanisms of the vibrational levels.

Argon is used as a diluent for temperature control. An optimum concentration of Ar is found that maximizes pulse energy, and at low concentrations of initial F, an optimum concentration of Ar is found for maximizing pulse duration.

Pulse duration decreases with increasing initial  $F_2$  dissociation, while an optimum dissociation of  $F_2$  is found that maximizes the pulse energy.

The effect of varying the initial temperature of the reactants on the pulse energy is small. An increase in the initial temperature decreases the pulse duration, as expected.

An  $H_2$ -rich mixture is desirable to provide an increase in pulse energy and pulse duration. The effect of varying the initial  $H_2$  concentration for  $H_2$ -rich mixtures is small.

The variations of the more uncertain rate coefficients at the time of this study reveal that the pulse characteristics are sensitive to changes in the total pumping reaction rates and to the distribution of pumping in the vibrational levels. These characteristics are not very sensitive to changes in the VV rates of  $HF(v)$  with  $HF(v')$  or  $H_2(v'')$ . The major effect of these changes is redistribution of energy emitted by the lasing bands.

## REFERENCES

1. D. J. Spencer, T. A. Jacobs, H. Mirels, and R. W. F. Gross, Intern. J. Chem. Kinet. 1, 493 (1969).
2. T. A. Cool, R. R. Stephens, and T. J. Falk, Intern. J. Chem. Kinet. 1, 495 (1969).
3. J. R. Airey and S. F. McKay, Appl. Phys. Letters 15, 401 (1969).
4. J. R. Airey, J. Chem. Phys. 52, 156 (1970).
5. G. Emanuel, Analytical Model for a Continuous Chemical Laser, Technical Report TR-0059(6240-20)-3. The Aerospace Corporation (September 1970). Also, to appear in J. Quant. Spectr. Radiat. Transfer.
6. R. L. Kerber and J. S. Whittier, The Effect of Various Parameters on the Behavior of the Pulsed HF Chemical Laser, Technical Report TOR-0059(6753-10)-1, The Aerospace Corporation (December 1970).
7. N. Cohen, T. A. Jacobs, G. Emanuel, and R. L. Wilkins, Intern. J. Chem. Kinet. 1, 551 (1969).
8. M. S. Dzhidzhov, V. T. Platonenko, and R. V. Khokhlov, Sov. Phys. Uspekhi 13, 247 (1970).
9. G. Emanuel, W. D. Adams, and E. B. Turner, Resale-1: A Chemical Laser Computer Program, Technical Report TR-0172(2776)-1, The Aerospace Corporation (July 1971).
10. D. E. Mann, B. A. Thrush, D. R. Lide, J. J. Ball, and N. A. Acquista, J. Chem. Phys. 34, 420 (1961).

11. In reality, stimulated emission buildup time is of the order  $2L/c = 6.6 \times 10^{-9}$  sec, which is small on the  $\mu$ sec time scale of the figure.
12. N. Cohen, A Review of Rate Coefficients for Reactions in the  $H_2 - F_2$  Laser System, Technical Report TR-0172(2779)-2, The Aerospace Corporation (July 1971).

## APPENDIX

### THE REACTION SYSTEM

The chemical kinetic model and corresponding rate coefficients used in this study are listed in the following table. Chemical rate coefficients for the HF laser system are from a compilation prepared by N. Cohen of our laboratory in December 1970. Subsequently, Cohen has reported a more final review of these rates.<sup>12</sup> Implications of the difference in rates between the table and Ref. 12 are not serious and are covered in the discussion. Some of the catalytic species listed at the bottom of the table are multiplied by a constant. This is equivalent to using a rate coefficient whose value is larger by this factor. The thermodynamic data are taken from the JANAF (Joint-Army-Navy-Air Force) publication distributed by Dow Chemical Corporation. However, the thermodynamic data of excited species are generated at this laboratory.

# Table of Reactions and Rate Coefficients

Reaction No.	Reaction <sup>1</sup>	Rate Coefficient <sup>2</sup>
1	$H_2(0) + M_2 \rightleftharpoons H + H + M_2$	$k_{-1} = 10^{18} T^{-1.0}$
2 <sup>3</sup>	$F_2 + M_4 \rightleftharpoons F + F + M_4$	$k_2 = 5.0 \times 10^{13} e^{35.30}$
3, ..., 6	$HF(v) + M_4 \rightleftharpoons H + F + M_4$	$k_{3+v} = 1.2 \times 10^{19} T^{-1.0} e^{135.80} \quad v = 0, \dots, 3$
7	$F + H_2(0) \rightleftharpoons HF(0) + H$	$k_7 = 9.0 \times 10^{12} e^{1.60}$
8	$F + H_2(0) \rightleftharpoons HF(1) + H$	$k_8 = 2k_7$
9	$F + H_2(0) \rightleftharpoons HF(2) + H$	$k_9 = 10k_7$
10	$F + H_2(0) \rightleftharpoons HF(3) + H$	$k_{10} = 5k_7$
11, 12, 13	$F + H_2(0) \rightleftharpoons HF(v) + H$	$k_{-7-v} = 10^{12} T^{0.670} \quad v = 4, 5, 6$
14	$H + F_2 \rightleftharpoons HF(0) + F$	$k_{14} = 6.0 \times 10^{14} e^{2.40}$
15	$H + F_2 \rightleftharpoons HF(1) + F$	$k_{15} = k_{14}$
16	$H + F_2 \rightleftharpoons HF(2) + F$	$k_{16} = 1.5k_{14}$
17	$H + F_2 \rightleftharpoons HF(3) + F$	$k_{17} = 2.66667k_{14}$
18	$H + F_2 \rightleftharpoons HF(4) + F$	$k_{18} = 3.33333k_{14}$
19	$H + F_2 \rightleftharpoons HF(5) + F$	$k_{19} = 5.5k_{14}$
20	$H + F_2 \rightleftharpoons HF(6) + F$	$k_{20} = 5k_{14}$
21, 22	$H_2(v) + M_1 \rightleftharpoons H_2(v-1) + M_1$	$k_{20+v} = 2.5 \times 10^{-4} v T^{4.3} \quad v = 1, 2$
23, ..., 30	$HF(v) + M_3 \rightleftharpoons HF(v-1) + M_3$	$k_{22+v} = 9.0 \times 10^8 v T^{1.30} \quad v = 1, \dots, 8$
31, ..., 38	$HF(v) + M_6 \rightleftharpoons HF(v-1) + M_6$	$k_{30+v} = 5.0 \times 10^7 v T^{1.30} + 10^{16} v T^{-1.43} \quad v = 1, \dots, 8$
39, ..., 46	$HF(v) + M_5 \rightleftharpoons HF(v-1) + M_5$	$k_{38+v} = 1.3 \times 10^{-2} v T^{3.60} \quad v = 1, \dots, 8$
47, ..., 53	$2HF(v) \rightleftharpoons HF(v-1) + HF(v+1)$	$k_{46+v} = 4.0 \times 10^5 T^{2.2} \quad v = 1, \dots, 7$
54, ..., 59	$HF(v) + HF(v+1) \rightleftharpoons HF(v-1) + HF(v+2)$	$k_{53+v} = 1.2 \times 10^3 T^{2.80} \quad v = 1, \dots, 6$
60, ..., 64	$HF(v) + HF(v+2) \rightleftharpoons HF(v-1) + HF(v+3)$	$k_{59+v} = 6.0 \times 10^{-2} T^{3.90} \quad v = 1, \dots, 5$
65, 66	$HF(v) + H_2(v-1) \rightleftharpoons HF(v-1) + H_2(v)$	$k_{-64-v} = 8.0 \times 10^5 T^{2.20} \quad v = 1, 2$
67	$HF(3) + H_2(0) \rightleftharpoons HF(2) + H_2(1)$	$k_{-67} = 1.2 \times 10^{-1} T^{3.90}$
68	$HF(2) + H_2(0) \rightleftharpoons HF(1) + H_2(1)$	$k_{-68} = 2.4 \times 10^3 T^{2.8}$

<sup>1</sup>Catalytic species:

$M_1 = H, F, Ar, HF(0), \dots, HF(8), 4^*H_2(0), 4^*H_2(1), 4^*H_2(2), F_2$   
 $M_2 = 20^*H, F, Ar, HF(0), \dots, HF(8), 2.5^*H_2(0), 2.5^*H_2(1), 2.5^*H_2(2), F_2$   
 $M_3 = F$   
 $M_4 = H, F, Ar, HF(0), \dots, HF(8), H_2(0), H_2(1), H_2(2), F_2$   
 $M_5 = H, Ar, H_2(0), H_2(1), H_2(2), F_2$   
 $M_6 = HF(0), \dots, HF(8)$

<sup>2</sup>The rate coefficients  $k_f$  and  $k_b$  designate forward and backward rates, respectively, with units in terms of moles, cm<sup>3</sup>, and sec. For each reaction, the missing rate coefficient is determined from the equilibrium constant.

<sup>3</sup>The quantity  $\theta = -(10^3/RT)$ , where the temperature  $T$  is in °K and  $R$  is 1.987 cal/mole-°K.

44